



## Introduction and Background

One of the more successful approaches to resolving dipolar degeneracies or couplings in solids NMR spectra has utilized correlations of anisotropic dipolar contributions with anisotropic chemical shift measurements, and one of the best ways to get the correlated data is the PISEMA technique.

Most prior NMR work on fully aligned membrane proteins has relied on mechanical alignment between flat plates, which (at lower fields) has often benefited from the use of flattened coils. However, the latest trends are toward the use of magnetic alignment in bicelles, often with a lanthanide inserted to cause them to align with their normals parallel to the polarizing field. With such samples, round coils are clearly better. Since the protein is necessarily quite dilute, the largest practical sample volumes are desired for maximum S/N, subject to the constraint of being able to achieve very high rf field strengths at three frequencies simultaneously at highest  $B_0$ .

The technical challenges arise largely from the requirement of very high rf field strengths during the  $^1\text{H}$ - $^1\text{H}$  CP, as well as the need for very high proton decoupling (and sometimes simultaneous  $^{13}\text{C}$  decoupling) during the signal acquisition period. RF heating exacerbates the problems at very high polarizing fields. Compromises in S/N have often been made to achieve higher RF field strengths. The general acceptance of the PISEMA and related high-power methods appears to be hampered by the lack of a fully satisfactory probe from commercial NMR probe vendors.

The objectives are a novel probe design for use in narrow-bore magnets that permits:

- (1) Maximum practical sample volume.
- (2) Much higher rf field strengths on all three channels simultaneously.
- (3) Higher efficiencies, especially on  $^{13}\text{C}$  and  $^{15}\text{N}$ .
- (4) Minimized decoupler heating.
- (5) Improved spectral resolution.
- (6) Availability of a z-gradient.

While we have shown that some of these objectives can be met with our "XC" coils as previously described, the high-field PISEMA and related techniques require that we push this technology to its limits with several major advances.

The advances being added to the prior XC technology include:

- (1) Utilization of balanced coils at all three frequencies simultaneously.
- (2) Use of a pressurized probe environment.
- (3) More effective control of lead inductance to the coils.
- (4) Ultra-low-loss transmission lines in a novel double-balanced circuit.
- (5) Development of novel, ultra-high-Q, high-power capacitors.
- (6) Improved magnetic compensation of the heavy solenoid.
- (7) Use of soluble amorphous teflon coatings.
- (8) An ultra-thin shielded z-gradient coil with transverse sample access.

## Maximum $^1\text{H}$ Decoupling with Minimum RF Heating

The rf power loss  $P_R$  in the sample is given by:

$$P_R = \int \sigma E^2 dV$$

where  $\sigma$  is the electrical conductivity,  $E$  is the electric field, and  $dV$  is a volume element. The E field satisfies the following,

$$\mathbf{E} = -\nabla\phi - \text{Grad } \phi_e$$

where  $\mathbf{A}$  is the magnetic potential vector field and  $\phi_e$  is the scalar electric potential due to electric charges.

It often comes as a surprise that for multi-turn solenoids the second term in the above equation may be an order of magnitude larger than the first term throughout the sample. Clearly, the solenoid cannot be used for the  $^1\text{H}$  in large, lossy samples at high fields.

While several methods have been shown to be useful in some applications for eliminating the E-field problem from the solenoid in large samples, the original "XC" (cross-coil) method developed and patented by Doty seems to be clearly the best for triple-resonance at high fields - especially where space is limited.

We routinely achieve 110 kHz  $^1\text{H}$  decoupling in the 4 mm XC probe at 750 MHz, and the limitation arises from the limited distance between the leads to the XC capacitors and the solenoid, not the chip caps, as the XC coil has extremely low inductance. A longer ceramic coilform can easily be used in the PISEMA probe (as it does not require MAS), which allows this clearance space to be doubled.

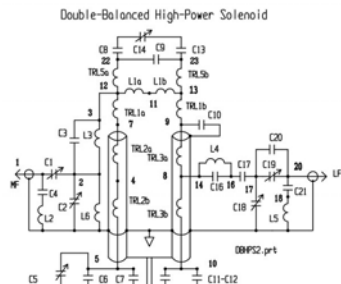
The weak link then becomes the 1 kV chip capacitors, even though 8 are used. We have identified a new source of chip capacitors with 1.5 kV ratings, and the low-value chips can be selected for even higher breakdown.

## A Novel Triple-balanced High-power Probe Circuit

It has often been argued that the use of transmission lines in place of some discrete components may permit higher rf field strengths. We have usually avoided deliberate replacement of lumped elements with transmission lines in our MAS probes for several reasons: (1) they severely limit multi-nuclear tuning; (2) they cannot be well adapted to the case where long leads to the sample coil are required for automatic sample exchange; (3) manufacturing costs are increased; and (4) transient response is degraded (stored rf energy is higher).

However, the situation is decidedly different in the PISEMA probe: (1) the probe tuning is fixed for  $^1\text{H}/^{13}\text{C}/^{15}\text{N}$ ; (2) automatic sample exchange is not provided; (3) a novel transmission-line circuit has been developed that permits much higher efficiency for the double-balanced  $^{13}\text{C}/^{15}\text{N}$  case than has previously been achieved; and (4) phase transients are not generally a significant problem in the PISEMA and related methods.

The double-balanced  $^{13}\text{C}/^{15}\text{N}$  transmission line circuit is shown below in Figure 3. (The separate,  $^1\text{H}$ -balanced XC circuit is quite similar to that described elsewhere).



The general behavior of the above LFMF circuit may be understood as follows. At the MF, ultra-low-loss coaxial lines TRL2 and TRL3 are each not much less than a quarter lambda. Hence, the low-impedance of the parallel high-power capacitors (C6-C7, C11-C12) at the lower ends of the TRLs is transformed into a high impedance (with balanced, differential voltage) at their upper ends. (Two parallel high-power 3.5 kV capacitors are used at the lower ends to achieve sufficiently low effective series resistance (ESR) and effective series inductance (ESL) as well as the needed current and voltage handling.) The sample coil (L1a, L1b) is approximately tuned with C9 (and its leads, TRL5) to the MF, thus presenting a high impedance at nodes 12,13 at the MF.

At the LF, C9 is of relatively little consequence, and the MF quarter-lambdas primarily add balanced tuning capacitance, supplemented by C6-C7 and C11-C12, to the sample coil. The sample coil is shown as two coils in series simply to place a node explicitly at its center, where the rf voltage is zero at both the LF and the MF. The inductance of approximately the lower half of TRL3 in series with C11-C12 results in near-zero impedance from node 8 to ground at the MF. Hence, the LF may be easily matched into this node with high MF isolation. Still, an MF trap, L4/C16, is added for further MF isolation. An equally convenient node for MF matching doesn't exist, so a hi-Q LF tank, C3/L3, is needed for adequate LF isolation of the MF matching circuit. HF traps C5/L2 and L5/C21 are sometimes needed.

It is not too difficult to achieve very low losses in all the tuning coils and capacitors other than C9. A first-pass approach is to use four 4 kV hi-power capacitors in a series-parallel arrangement here. However, we plan to use ultra-high-Q alumina capacitors similar to those we are developing for our CryoMAS probe for improved Q at the MF in the near future.

## Shielded Gradient Coil

Though not yet applied to the PISEMA experiment, gradients have proven essential in most other NMR techniques - for coherence selection, solvent suppression, and reduction in acquisition time in multi-dimensional spectra. This suggests gradients, if available, will also be useful in NMR methods for highly aligned membrane proteins. Moreover, the exceptional S/N of this probe will indicate its use for some solution applications (SOPAST,  $^{13}\text{C}$ -detected, etc) where gradients are routinely required.

There are a unique aspects to this probe which require the gradient coil to be of novel design. First, the coil and sample coil are oriented with their axis perpendicular to  $B_0$ . Secondly, the transverse rf coilform needs to be rather long - space is needed to accommodate very high voltages on both coils. Thirdly, the sample coils will be pressurized with nitrogen for increased power handling.

Hence, the gradient coil must be as thin as possible and have a transverse sample access port that still easily allows the rf coils to be in a pressurized zone. Figure 5, to the right, shows the gradients in relation to the sample, its coils, and tuning region.

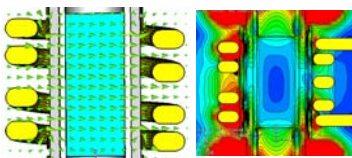
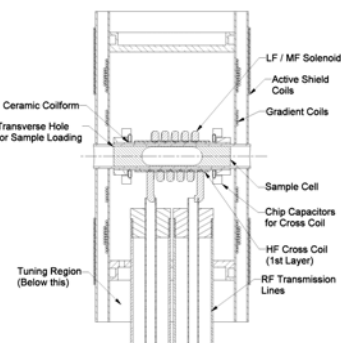


Figure 1 (left): H vector plot, YZ plane, for the XC coil. Note that the outer solenoid (used for the LF and MF) is not driven here, and the (driven) inner  $^1\text{H}$  XC is scarcely visible. Figure 2 (right): Plot of the E field magnitude from the XC at 750 MHz in the yz-plane for 17 contours from 0 to 8000 V/m.



Figure 4 (above): Photo of completed prototype. The shield body tube (with the gradient coil) seats around the sample access so the entire probehead can be pressurized for increased power handling. The quartz variable capacitor extending from the top is the coarse-tune adjustment for the MF. Fine-tune adjustments for all three channels are accessible from the bottom.



## Mitigation of High-Voltage Breakdown

The weak link in power handling in early versions of our MAS XC probes in NB high-field magnets was generally voltage breakdown between the inner HF XC and the outer solenoid. Balancing the MF and LF roughly doubles the voltage handling at either frequency individually. Additional voltage handling is obtained by lengthening the coilform to allow more space between the XC capacitors and the solenoid.

Another limitation arises from the teflon insulation between the  $^1\text{H}$  cross-coil and the outer solenoid used for the mid frequency (MF) and low frequency (LF). Compared to that normally used in our solids XC probes, the thickness of this insulation has been doubled (from 0.5 to 1 mm).

The rf breakdown voltage in gases at pressures in the 0.3 to 0.3 bar range is nearly linear with gas pressure, so pressurizing the coil environment (even to only 0.25 MPa) is very beneficial. This, of course, introduces a number of challenges, not the least of which is sealing around all the rf lines, tuning adjustments, and sample access. Pressurized operation will be particularly essential as we go to higher fields.

To achieve high  $B_0$  homogeneity, closely spaced turns are needed in L1, especially at the ends. Still, breakdown between turns is not a problem, except where rf heating of the epoxy bonds leads to surface tracking. We have found that loading the epoxy with powdered silicon nitride (and C60, for magnetic compensation) helps, but it is still essential to limit its use to the thinnest possible film.

The use of massive conductors where currents are high is essential to limit pulse heating, as breakdown voltage in gases decreases with T. The rf solenoid wire, as shown in cross-section in Fig. 1 (about 1.4 mm x 2 mm) is edge-wound with sufficient space between turns for optimum performance of the  $^1\text{H}$  XC. The solenoid's wire size is somewhat limited by susceptibility compensation errors and their effect on resolution and lineshape. The PISEMA probe does not benefit from MAS, so magnetic compensation of its solenoid wire is actually more critical than in HR-MAS. To use a heavier wire without degrading resolution will require improved compensation accuracy. Mean net susceptibility is currently about 24% that of copper. We expect to improve compensation accuracy in the future, which will allow us to use heavier wire and simultaneously achieve better resolution.

Finally, we have found that voltage handling can be improved by application of a thin coating of soluble amorphous Teflon to the sample coil in our standard MAS-XC probes.

## Preliminary NMR Test Results

The following measurements, at moderate power levels, confirmed efficiencies:

$^1\text{H}$ , 500 MHz, 128 V,  $\text{pw}90 = 2.7 \mu\text{s}$ .

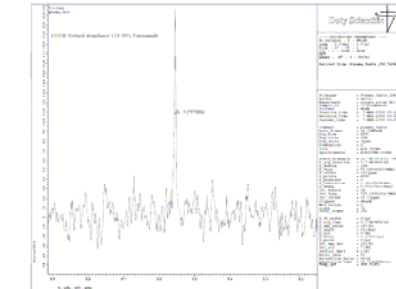
$^{13}\text{C}$ , 125 MHz, 650 V,  $\text{pw}90 = 4.5 \mu\text{s}$ .

$^{15}\text{N}$ , 50 MHz, 1500 V,  $\text{pw}90 = 3.8 \mu\text{s}$ .

The proton and carbon channels are expected to handle about twice the power used in the above tests, but shortness of time prevented those tests from being carried out. The probe shimmed to about 14 Hz FWHM with good lineshape on  $^1\text{H}$  on a chloroform cylindrical sample with a small air bubble. Using a special cell that allows elimination of the air bubble and susceptibility matching should permit much better resolution.

The natural abundance  $^{15}\text{N}$  S/N on 70  $\mu\text{l}$  of 90% formamide in DMSO was measured to be 12:1 for 40 scans with 50 kHz decoupling. (The  $^{15}\text{N}$  spectrum shown below was for fewer scans with some parameters not optimized.)

The electronics region was pressurized with  $\text{N}_2$  to 21 psi during NMR measurements. Bench tests showed voltage breakdown beginning at 1200 V (at  $^{15}\text{N}$ ) in the absence of coil pressurization.



## Conclusions

The combination of pressurizing the electronics region and balancing the circuits at all three frequencies permits the attainment of much higher rf field strengths on all channels simultaneously in a narrow-bore, high S/N probe for use with large samples at highest fields.

## REFERENCES

1. F. D. Doty, "Probe Design and Construction," *Encyclopedia of NMR*, Wiley, 2007.
2. F. D. Doty, G. Entzminger, and A. Yang, "Magnetism in HR NMR Probe Design, Part II: HR-MAS," *Concepts in Magn. Reson.*, (4), 239-260, 1998.
3. F. D. Doty, J. Kulkarni, C. Turner, G. Entzminger, A. Bielecki, "Using a cross-coil to reduce RF heating by an order of magnitude in triple-resonance multinuclear MAS at high fields", *J. Magn. Reson.*, 182 (2006), 239-253.

Acknowledgements: This work supported by NIH R43 GM079888-01.